Grenze International Journal of Engineering and Technology, June Issue

Immunotheraphy for Breast Cancer by Immune Check Point Inhibitors (Pd-1 & Pd-L1) using CNN for Image Analysis in Deep Learning

Abila.R[1], Ranjith kumar. P[2] and Reeta Ruby R[3]
[1]PSR Engineering college/ Applied Electronics, Virudhunagar,India.
Email: abila61999@gmail.com
[2]Associate Professor, PSR Engineering college, Virudhunagar,India.
Email: ranjithkumar@psr.edu.in
[3]ECG Analayst , CHC Healthwatch Chennai
Email : reetaruby2001@gmail.com

***Abstract*— The second most endemic cause of mortality for women is breast cancer. Therefore, any advancements in cancer forecasting and analysis are critical to a balanced life, and high accuracy cancer predictions are crucial to updating patient viability and treatment options. As a result, early identification that is accurate can lower the incidence of breast cancer. The basic idea behind CNNs (Convolutional Neural Networks) is to employ hyperplanes to distinguish between different groups and further improve the diagnostic system's performance. Deep learning methods have been shown to be resilient and can significantly aid in the prediction and early diagnosis of breast cancer. They can also serve as a hub for research. It has recently been proposed that programmed death ligand-1 (PD-L1) serves as a prognostic biomarker for the treatment of breast cancer. The immunohistochemistry (IHC) measurements of PD-L1 rate, duration, and variability are shown last. Hematoxylin and eosin (H&E), on the other hand, is a potent dye that is widely employed in the diagnosis of cancer. Here, we demonstrate that by limiting the deep learning procedure in this instance, PD-L1 expression may be anticipate from images stained with H&E. Our technique calculated the PD-L1 area under the curve (AUC) to be 0.99 in a cohort of 500 individuals. Our technology performs consistently and has been verified using outside data, including hacking tests.**

***Index Terms*— Breast Cancer ,Deep Learning, CNN, ResNet Architecture, Check point Inhibitors.**

I. INTRODUCTION

In 2021, breast cancer will be the primary cause of mortality for women between the ages of 20 and 60, making for 12% of all newly diagnosed cancer cases globally. Two of the most promising recently developed treatments for many cancer types are targeted immunotherapies against programmed death ligand 1 (PD-L1) and programmed death 1 (PD-1). By stopping the immune system from interfering with the interaction between PD-L1 and the PD-1 checkpoint, these medications aid the immune system. When it comes to overall response and survival, immunotherapy with PD-L1/PD-1 inhibitors is better to normal chemotherapy in cancer patients whose tumour cells express more than 50% PD-L1. While PD-L1 has lately drawn interest as a population immune response

Grenze ID: 01.GIJET.10.2.843

biomarker in triple-negative breast cancer patients, chemotherapy did not enhance overall survival in these patients. This is due to the fact that it works well in treating lung cancer among other cancer forms. Restricting our focus to patients who test positive for PD-L1, immunotherapy may increase survival. The FDA approved the use of immunohistochemistry (IHC) with Ventana SP142 staining to assess PD-L1 in patients with triple-negative breast cancer in order to identify which patients should get immunisation based on the findings of this research. Detection of PD-L1 by IHC is now the gold standard for PD-L1 testing; nevertheless, it is costly, time-consuming, potentially tissue-damaging, and may not even be accessible in some nations or locations. Its analysis is difficult, knowledge-based, and frequently unreliable. There are several ways to stain PD-L1, and research has demonstrated that the staining methods and antibodies employed can impact how well PD-L1 measurements work. Even when staining is done alone, other research has demonstrated that the validity of PD-L1 evaluation by trained physicians is reduced.

II. H&E,Tissue Microarray (TMA) Images In Breast Cancer

It is demonstrated here that CNN-based scanning of H&E pictures may be able to envision PD-L1 expression. This makes it difficult to obtain significant amounts of data of H&E pictures minted with PDL1 utterance. PD-L1, albeit newly identified as a useful biomarker in breast cancer, is not commonly employed in clinical practice. A sizable tissue microarray library that included H&E-stained pictures together with other comparable stains for additional biomarkers, such as IHC for PD-L1, was used in our investigation. An experienced pathologist annotated the samples in the collection for PD-L1 expression. Thanks to the dataset we collected, we were able to train and assess a CNN for the first time for the prediction of PD-L1 utterances from H&E images. Breast Cancer Wisconsin Diagnostic (BCWD) collection includes tissue samples, clinical and pathological data, and 26,763 TMA pictures from 5596 patients. Figure 1 summarises these TMA images.

A. PD-L1 in the BCWD Cohorts

The study's foundation was provided by the Breast Cancer Wisconsin Diagnostic (BCWD) in (Fig.1), which supplied tissue samples and clinic pathological data from 26,763 TMA images of 5596 patients. The BCW cohort is made up of 4,944 American women whose tumour exhibits were examined by a central laboratory and who had their initial diagnosis of invasive breast cancer between 1986 and 1992. Every woman provided three H&E-stained TMA cores, one IHC-stained TMA for PD-L1, and one for PD-1. To analyse the complete data, which included both BCWD cohorts, PD-L1 positive (or) negative condition, an experienced pathologist reviewed every accessible H&E and PD-L1 TMA picture Figure (1)-D1, D2, D3,... shows the patient sample collection data.

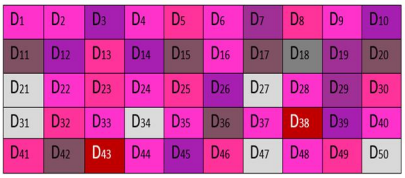

Fig.1 TMA images (BCWD).

B. Training and Testing the System

We precompute the TMA pictures stained with H&E by scaling and cropping each image from a resolution that matches the data for training and assumptions. To improve the model's ability to account for differences in griminess between cohorts, the prints were resized and cropped to 512 × 512 pixels. Additionally, an analysis of missing data was done. The BCWD instances at the patient position were arbitrarily divided into training (2500,74.5) and test (865,25.5) sets (Fig. 2). The training set was further suitably divided into five train and confirmation crowds at the patient position using 5-fold cross-validation (CV).We randomly selected the patient sample data for the training and testing sets in Figure (2).

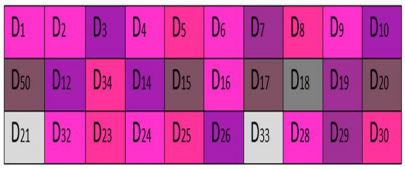

Fig.2 Testing and Training set

III. Proposed Methodology

Because the form of the excrescence, as captured by the H&E colour, provides a portending signal for the molecular provider position of the excrescence, a machine literacy (ML) system may immediately descry ERS from an H&E stained whole slide image (Fig. 1). The biology is reflected in the morphology; in this instance, the biology may require modifications to the expected cell arrangement and dependence on hormone signalling.
We show that ML can identify groups of histo morphological characteristics in the towel structure that are indicative of the molecular biomarkers or biology shown by an IHC stain and captured by an H&E colour. There are several of advantages to working with H&E.It is widely used in histopathology procedures worldwide, is significantly less expensive than IHC, and exhibits less variation between centres.
An automated ERS computing method speeds up decision-making while also improving outcomes and reducing crimes in the treatment of bone cancer. Additionally, a system that recognises morphological traits for molecular pointers might provide scientific details regarding the ways in which hormones stimulate the growth of excrescences.

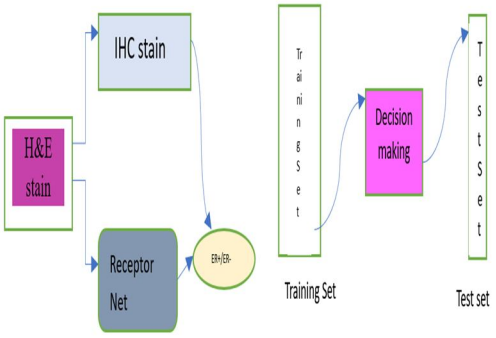

Fig.3 Data Annotation Process

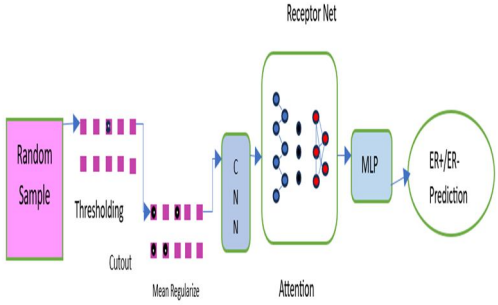

Fig.4 Training and Inference

Furthermore, we trained a single model with the same armature, silhouettes, hyperparameters, and age range across the whole training set. The system was then verified using this model on an independent test set that was left out of the cross-validation. This led to a PD-L1 vaticination outgrowth in each of the 860 test cases. For the BCWD test set, the AUC performance was 0.99 (99).

A. CONVOLUTIONAL NEURAL NETWORK

Convolutional neural networks are a subclass of machine literacy. It's one of the many variations of artificial neural networks that are fascinated by various types of information and purposes. A CNN is a kind of network architecture that is particularly helpful for tasks involving the interpretation of pixel input, like as image recognition, according to deep literacy methods. Although there are different types of neural networks, CNNs are the preferred network architecture for item identification and recognition in deep literacy applications. For tasks requiring object recognition, such as facial recognition and tone-driven buses, they are therefore perfect for computer vision (CV) applications. CNNs are one of the most widely used types of neural networks, and they have been applied extensively to deep literacy, mostly with a lot of data (pictures and videos). The neurobiology of the cortex leads to the development of the multilayer neural network. This structure consists of completely linked and convolutional layers. Between these two layers, there might be subsampling layers. They obtain the best performance from DNNs with efficiently scalable complexity and multidimensional locally recognised input data. CNN is hence inflexibly applied in datasets with relatively high bump counts.

III. Results And Discussion

A. Computer aided application for fast annotation

To achieve a fast and precise annotation process, we created a computer software for PD-L1 and PD-1 annotation based on our solutions for all patient H&E and IHC-stained TMA images. To flip between the patients, between H&E and similar IHC images of the same patient, a conscientious button was utilised. The pathologist has seven reasonable options to select from in each case: ‘Negative,’ ‘Positive,’ ‘No TMA,’ ‘No tissue,’ ‘No tumour,’ ‘Deficient staining,’ & ‘Out of focus.’ When a label button was pressed, the display pane was instantly tinted with a distinctive hue to help users recognise the selected label and prevent confusion or errors. Other buttons were included to direct users to prior patients, provide them the option to annotate in specific situations, and save their

inputs for potential future use. The pathologists were not allowed access to patient IDs or other sensitive information in order to prevent inciting bias.

B. Data pre-processing and augmentation

Initially, a 1440 × 1440 square segment was cut from the centre of every TMA picture. While the squared part was locked to the centre of the image's 1440 x 1440 pixels before assumption, it was randomly clipped from inside the image's 1640 × 1440 central section during training. It was predicted that this random crop approach would strengthen the model against variations in the tissue's placement, which is not always exactly centred, on the scanned slides. Next, the resolution of each image was reduced to 512 × 512. The model was then assisted in addressing the variability in staining techniques and within cohorts through the use of data augmentation. In particular, we executed colour jittering and inadvertently turned and inverted each image. Gamma correction, temperature and saturation jittering, additive Gaussian noise, and garble augmentations were all incorporated in the colour jittering. Throughout the interpretation process, no data augmentations were used.

C. Convolutional Neural Network-ResNet Architecture

We trained and tested the model using a CNN containing residual connections resulting from the ResNet architecture (Supplementary Figure 1). BatchNorm layer, ReLU activation layer and the first layer activation layer for the CNN model. The input is then encoded into vectors embedded in the R256 internal space using a CNN architecture consisting of four blocks. After the 2-step convolution layer, each CNN block has a spatial subsampling function equipped with three 1-step convolution layers. Each convolutional layer has a 3 x 3 kernel, followed by a BatchNorm layer and a ReLU activation function. After down-sampling, the slice contains the input and output of each block. At the end of the block, we use averaging to compress the final description of the input image to a vector of size 1×256. Then, a 256 × 2 linear layer is used to split the embedding vectors into specific labels. The output vector of dimension 2 is then passed to the SoftMax output to determine the result of the final class containing the final result for each label. The total sample contains 2,755,538 parameters. Due to the difference in recording data, we decided to use Focus Loss as a learning target. Unintended biases can occur when inadequate training material is pushed into deep channels using noisy competition. The network will have a fair chance to learn to handle negative class instead of data distribution. This problem is solved by focal loss, which replaces traditional cross-entropy to reduce the loss applied to identified samples. Focus loss focuses training on complex situations and prevents the network from being frightened by a large number of incorrect numbers during training, thus improving analysis and reducing unfairness.

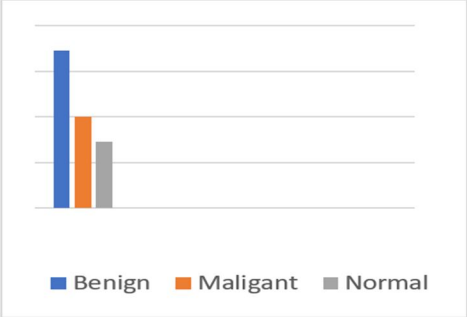

Fig.5 Stages predicted as benign, normal classes and malignant

D. Training & Testing Split

We need to take into account a few factors before dividing our data. The first is the proportion of malignant to non-cancerous photos in our database. We discovered before that there is not a consistent divide in our data. We may have a biassed model since we have a large number of non-cancerous photos.In every experiment, we used the identical hyperparameters. We utilised the RAdam optimizer to experience every model.This might potentially be problematic when assessing our model. Assume, for the sake of extreme argument, that our model classified our entire dataset as cancerous (i.e., 90 out of 100 points are cancerous and 10 are not). This would result in an accuracy of 90%, but it is not really representative of what is actually happening. Actually, it consistently misclassifies our data that is not malignant.We may divide our data using the traintest split function provided by sklearn model_selection, This, when grouped by the classes, enables us to produce training and testing sets that are uniformly dispersed.

Analytical Analysis

Data creation, annotation, and analysis took place between July 1, 2015, and February 1, 2022. The following analytical measures were used: Cohen's kappa, area under the curve (AUC), specificity, sensitivity (=recall), negative predictive value (NPV), and positive predictive value (=precision). The receiver operating characteristics (ROC) curves shown as False Positive Rate vs True Positive Rate. Bootstrapping was used to compute the dependence intervals. An analytically significant result was obtained using a 1-tailed hypothesis test with $P < 0.05$. The accuracy was evaluated using a threshold that was best established by utilising the BCWD training data after the scores had been converted to binary. For the sole purpose of predicting the PD-L1 status, a logistic regression was fitted for each variable in order to perform the single-variable analysis. For the multivariate analysis, an L1-regularized logistic regression was run on each variable as a whole using the BCWD training data.

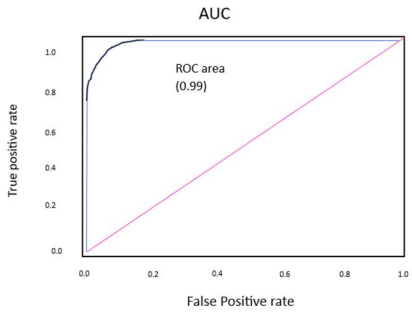

Fig.6 AUC of BCWD

E. Preception by t-SNE distribution

During the interpretation stage, we extract the features of the final CNN layer for every H&E-stained TMA picture in order to produce the t-SNE perception. The feature vector from each patient's H&E picture had the greatest prediction score was then used to represent that patient. The feature vectors were then processed using t-SNE to provide a 2D representation for every patient.

TABLE I COMPARISON OF T-SNE AND PCA

Criteria	**t-SNE**	**PCA**
Method	Non-Linear	Linear
Computation	Expensive	Less
Stability	May Vary	Stable
Usage	Visualization	Data
Assumptions	None	None
Sensitivity to	High	Low

F. Output Predicted as Randomly as Malignant,Benign

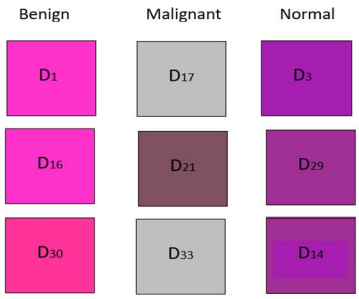

The finest model to be used for observing breast cancer as found in this review is the CNN. It gives a prediction accuracy of ~99% for the test data set.

IV. Conclusion

To the best of our knowledge, the majority of the patients were classified as low-PS users. Moreover, it is well recognised that IHC staining may not always be enough. It's also likely that some of the rare instances that pathologists were positive for without a doubt were really PD-L1 negatives due to overstaining or other staining inadequacies. These staining inaccuracies could have gone unnoticed by the algorithm, which predicated its prediction on the intense H&E staining. This interpretation underscores the system's potential use as a quality affirmation in clinical practice by indicating situations that may be more ambiguous and require more testing or retention.

The variation amongst pathologists may potentially indicate that the system's prognosis was not entirely accurate based on the ground truth annotation. We changed the prediction performance and removed the patient data (four instances in the low-PS group in BCWD) from the research when the pathologists could not concur. The outcome was an increase in the AUC performance from 0.99 on the BCWD test set. The BCWD-test data was filtered to exclude only instances from the low-PS positive group, thus even if performance increased dramatically, the resultant AUC could be biassed. The sensitivity and NPV of the BCWD-test set (BCWD-test-con) increased from 0.943 to 0.971 and 0.983 to 0.991, respectively. This suggests that the system's predictions based only on H&E pictures could be missing important information that could help doctors make better judgements. Before receiving FDA clearances or thorough validations, this kind of technology might be employed as a quality assurance and reannotation suggestion tool for PD-L1 reinterpretation or even restaining.

References

[1] Gil Shamai,Amir Livne,Antonio Polonia,Edmond Sabo,Alexander Cretu,Gil Bar-Sela &Ron Kimmel," Deep Learning based image analysis predicts PD-L1 status from H&E-stained histopathology in breast cancer",Nature Communication, 08 November 2022, doi.org/10.1038/s41467-022-34275-9

[2] Essam H. Houssein, Marwa M. Emam," Deep and machine learning techniques for medical imaging-based breast cancer",Elseiver,Vol : 2020.

[3] Ranjini K; Mouleeswaran S K," Breast Cancer Prediction by Leveraging Machine Learning and Deep learning Techniques with Different Imaging Modalities", Publish: IEEE Xplore,Published on: 18 July 2022.

[4] Li Tong;Ying Sha,May D Wang," Improving Classification of Breast Cancer by Utilizing the Image Pyramids of Whole-Slide Imaging and Multi-scale ConvolutionalNeural Networks", Publish: IEEE Xplore,Published on:09 July 2021.

[5] Sheryas Malakarjun Patil,Li Tong,May Di Wang," Generating Region of Interests for Invasive Breast Cancer in Histopathological Whole-Slide-Image", Publish:IEEE Xplore,Published on:22 Sep 2020.

[6] Dmitrii Bychkov, Nina Linder," Deep learning identifies morphological features in breast cancer predictive of cancer ERBB2 status and trastuzumab treatment efficacy", Scientific Reports Review Article,Published: 17 February 2021.

[7] Tsung-Yi Lin,Priya Goyal," Focal Loss for Dense Object Detection", Publish: IEEE Transaction,Published: 25 Dec 2023.

[8] Akinboro.O, FDA Approval Summary: Pembrolizumab, Ate- zolizumab, and Cemiplimab-rwlc as single agents for first-line treatment of advanced/metastatic PDL1 high NSCLC. Clin. Cancer Res. https://doi.org/10.1158/1078-0432.CCR-21-3844 (2023)

[9] Bray.F, Global cancer statistics 2018: GLOBOCAN estimates of incidence and mortality worldwide for 36 cancers in 185 countries. CA Cancer J. Clin. 68, 394–424 (2023).

[10] Ehteshami Bejnordi, B., Using deep convolutional neural networks to identify and classify tumor-associated stroma in diagnostic breast biopsies.